# Grid Factor and Solar Share Determine Ferry Electrification $CO_2$ Reductions: A Two-Variable Analysis

Sandith Thandasherry[1]

[1]CEO, Navalt, India. Email: sandith@navalt.in

June 2026

**Abstract**

Electrification of inland and coastal passenger ferries is widely promoted as a decarbonization strategy. But replacing onboard diesel combustion with shore-supplied grid electricity shifts the emission source rather than removing it, and on grids with high carbon intensity the substitution can increase total $CO_2$ emissions. This note extends the cost-of-energy framework of my earlier work [1] to $CO_2$ accounting. I derive a closed-form expression for the $CO_2$ reduction from replacing a diesel ferry with a battery-electric ferry, in just two variables: the grid carbon factor $g$ ($\mathrm{kg\,CO_2/kWh}$) and the share $s$ of daily energy supplied by onboard solar. The result is independent of vessel size, route, and operating profile. The propulsion break-even reduces to $g(1-s) < 0.76$. Auxiliary loads, met on a diesel vessel through a generator set, tolerate a dirtier grid still (break-even $\approx 0.94$). I map both thresholds against representative national grid mixes.

**Keywords:** ferry electrification; well-to-wake $CO_2$; specific fuel consumption; solar PV; grid carbon intensity

## 1 Introduction

Coastal and inland passenger ferries are an attractive early target for maritime decarbonization. Operating profiles are predictable, energy demand per voyage is bounded, and overnight shore charging is feasible at fixed berths. In an earlier paper [1] I developed a cost-of-energy framework for ferries, in which the OPEX gap between a diesel and an electric vessel is governed by the spread between fuel cost and grid cost. That analysis showed auxiliary energy costs fall faster than propulsion costs under electrification — a structural consequence of the drivetrain, independent of grid mix — and that solar contribution and hybrid topology (parallel versus series) further reshape the OPEX picture. Here I extend the framework from cost to $CO_2$ emissions, deriving an analogous closed-form expression in the grid carbon factor $g$ and onboard solar share $s$.

Several case studies have demonstrated the economic viability of battery-electric ferries in specific operating contexts [2–5]. Figure 1 reproduces the generalized powertrain topology of that cost-of-energy framework [1], in which several energy sources — electrical sources feeding a common bus, alongside purely mechanical paths — meet a single propulsion energy demand. The present analysis specializes this topology to the two pathways of interest for $CO_2$ accounting: the diesel-engine reference and the grid-plus-solar battery-electric case. However, the underlying $CO_2$ accounting depends critically on the source of the replacement electricity. Where the grid is dominated by coal or other high-carbon fuels, the apparent benefit of replacing a well-to-wake diesel chain with grid-supplied electrons may diminish or reverse.

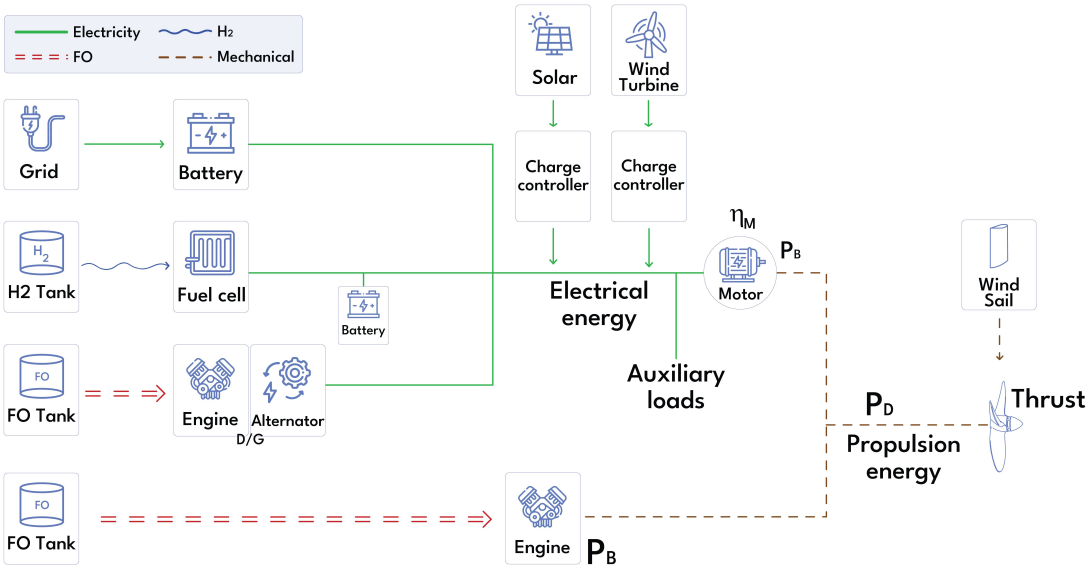


Figure 1: Generalized ferry powertrain topology, reproduced from the cost-of-energy framework of [1]. Five electrical generation sources — grid charging, a hydrogen fuel cell, a diesel–generator (D/G) set, solar PV, and a wind turbine — feed a common electrical bus that supplies auxiliary loads and the propulsion motor (efficiency $\eta_M$, brake power $P_B$). Purely mechanical propulsion paths (direct diesel engine and wind sail) are shown dashed. The present note specializes this topology to the diesel-engine reference and the grid-plus-solar battery-electric case.

This note isolates the $CO_2$ comparison between a diesel reference and a battery-electric ferry with onboard solar augmentation. I adopt well-to-wake (WTW) accounting symmetrically for both sides — upstream production plus combustion for diesel, and upstream generation for grid electricity — consistent with the conventions of the IMO LCA Guidelines [7]. Embodied (manufacturing) emissions are excluded on both sides of the comparison. As shown in [6, pp. 25–26], the production emissions of the solar array, battery, and associated equipment are offset within roughly one year of operation — a small fraction of a vessel's multi-decade operating life — while the embodied emissions of the diesel engine and its accessories are likewise minor, and structural components common to both vessels cancel. The comparison here is therefore confined to operational, well-to-wake energy. The contribution is a single closed-form inequality describing the $CO_2$ break-even surface, and a quantitative mapping of representative grid mixes onto that surface.

# 2 Model

## 2.1 Diesel reference

The annual mechanical propulsion energy demand $E_{\text{mech}}$ (kWh/yr) is supplied by combustion of marine diesel with specific fuel consumption $SFC$ (g/kWh), density $\rho$ (kg/L), and well-to-wake emission factor $f_d$ (kg $CO_2$/L, upstream plus combustion). The diesel reference pathway is shown in Figure 2; well-to-wake annual emissions are:

$$\mathrm{CO}_2^{\text{diesel}} = E_{\text{mech}} \cdot \frac{\mathrm{SFC}}{1000 \cdot \rho} \cdot f_d \quad [\text{kg CO}_2\text{/yr}] \tag{1}$$

Adopting representative values SFC = 250 g/kWh, $\rho = 0.85$ kg/L, and $f_d = 3.20$ kg $CO_2$/L (a well-to-wake factor: IMO/IPCC tier-1 combustion for marine gas oil [8], plus ∼19% upstream

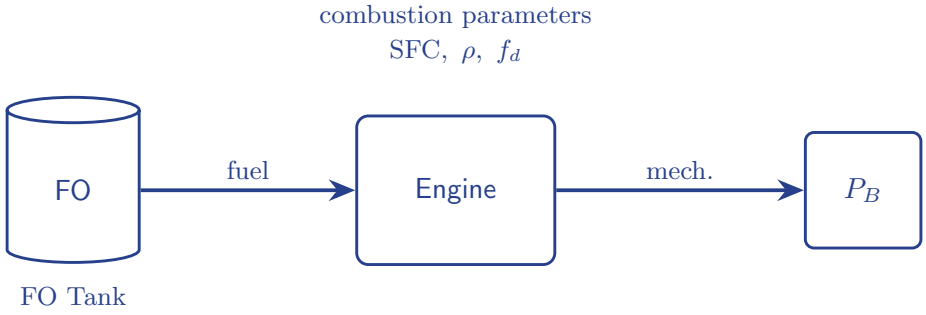


$$\mathrm{CO}_2^{\mathrm{diesel}} = E_{\mathrm{mech}} \cdot \frac{\mathrm{SFC}}{1000\,\rho} \cdot f_d \;\; [\mathrm{kg\,CO_2/yr}]$$

Figure 2: Diesel reference pathway. Fuel oil from the tank is combusted in the engine — characterized by specific fuel consumption SFC, density $\rho$, and emission factor $f_d$ — to deliver brake power $P_B$, i.e. the mechanical propulsion energy $E_{\mathrm{mech}}$ at the propeller. The resulting well-to-wake annual emissions are given by equation (1). Pathway adapted from the cost-of-energy framework of [1].

extraction, refining, and distribution [11]):

$$\mathrm{CO}_2^{\mathrm{diesel}} \approx 0.941 \cdot E_{\mathrm{mech}} \quad [\mathrm{kg\,CO_2/kWh_{mech}}] \tag{2}$$

Equation (2) is the diesel WTW carbon intensity per unit of mechanical propulsion energy delivered. It is independent of vessel size, route, and operating schedule, provided the engine operates near its design point.

## 2.2 Electric reference (battery + solar)

Mechanical propulsion energy is delivered through a drivetrain comprising the electric motor (efficiency $\eta_M$), the onboard electrical and power-conversion systems (efficiency $\eta_e$), and the battery (efficiency $\eta_b$). Following the cost-of-energy framework of [1], the energy that must be drawn from the charging source to deliver $E_{\mathrm{mech}}$ at the propeller is therefore $E_{\mathrm{elec}} = E_{\mathrm{mech}}/(\eta_b\eta_e\eta_M)$. A fraction $s \in [0, 1]$ of this energy is supplied by onboard solar PV (assumed effectively zero-carbon at point of use, consistent with [1] equation (5) which assigns zero cost of solar energy); the balance $1 - s$ is drawn from the grid with carbon intensity $g$ ($\mathrm{kg\,CO_2/kWh}$). The electric reference pathway is shown in Figure 3; annual emissions are:

$$\mathrm{CO}_2^{\mathrm{electric}} = \frac{E_{\mathrm{mech}}}{\eta_b\eta_e\eta_M} \cdot (1 - s) \cdot g \tag{3}$$

With $\eta_b = 0.95$, $\eta_e = 0.95$, and $\eta_M = 0.90$ (combined drivetrain efficiency $\eta_b\eta_e\eta_M = 0.812$):

$$\mathrm{CO}_2^{\mathrm{electric}} \approx 1.231 \cdot E_{\mathrm{mech}} \cdot (1 - s) \cdot g \tag{4}$$

## 2.3 Emissions reduction

Defining emissions reduction $R$ as the fractional decrease in annual $\mathrm{CO_2}$ achieved by electrification:

$$R = 1 - \frac{\mathrm{CO}_2^{\mathrm{electric}}}{\mathrm{CO}_2^{\mathrm{diesel}}} = 1 - \frac{(1 - s) \cdot g}{\eta_b\eta_e\eta_M} \cdot \frac{1000 \cdot \rho}{\mathrm{SFC} \cdot f_d} \tag{5}$$

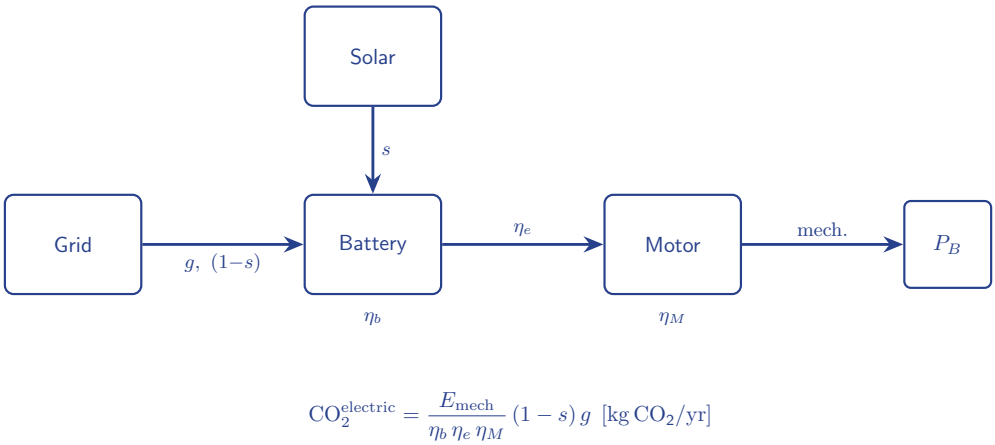


Figure 3: Electric reference pathway. Charging energy from the grid (fraction $1 - s$, carbon factor $g$) and onboard solar PV (fraction $s$, zero-carbon at point of use) is stored in the battery and delivered to the propeller through the drivetrain, incurring three efficiency drops: battery $\eta_b$, onboard electrical/power-conversion $\eta_e$, and motor $\eta_M$. Only the grid fraction carries $CO_2$, giving the annual emissions of equation (3).

Substituting numerical values:

$$\boxed{R = 1 - 1.308 \cdot g \cdot (1 - s)} \tag{6}$$

The vessel-specific term $E_{\mathrm{mech}}$ cancels, mirroring the cancellation of vessel-specific terms in the cost-of-energy analysis of [1]. Equation (6) holds for any vessel operating on any route at any service interval, subject to the underlying efficiency, density, and emission factor assumptions.

### 2.4 Break-even condition

Setting $R = 0$ gives the locus on which electrification is $CO_2$-neutral relative to diesel:

$$g \cdot (1 - s) = 0.764 \tag{7}$$

Above this locus electrification increases emissions; below, it reduces them.

### 2.5 Auxiliary loads

Equation (6) concerns propulsion energy, which the diesel reference delivers mechanically. Auxiliary loads (hotel power, HVAC, navigation) are instead electrical, and on a diesel vessel they are met by a diesel generator set — an engine driving an alternator of efficiency $\eta_A$. The genset therefore carries the full combustion intensity *plus* a mechanical-to-electrical conversion loss, whereas the battery-electric vessel supplies these loads through the battery and onboard electrical system but without the propulsion motor in the path. Writing the auxiliary reduction $R_{\mathrm{aux}}$ on a delivered-electrical-energy basis, only the motor term $\eta_M$ drops out (the battery $\eta_b$ and onboard electrical efficiency $\eta_e$ remain), and the alternator term $\eta_A$ enters in place of it:

$$R_{\mathrm{aux}} = 1 - \frac{\eta_A}{\eta_b\,\eta_e} \cdot \frac{1000\,\rho}{\mathrm{SFC} \cdot f_d} \cdot (1 - s)\,g \approx 1 - 1.06 \cdot g\,(1 - s), \tag{8}$$

taking the alternator efficiency equal to the motor, $\eta_A = \eta_M = 0.90$, with $\eta_b = \eta_e = 0.95$. The auxiliary break-even therefore lies at $g(1-s) \approx 0.94$, against 0.76 for propulsion (equation (7)). Auxiliary electrification thus tolerates a dirtier grid than propulsion: a vessel whose demand is part auxiliary has an effective break-even between these two values, weighted by the auxiliary share. This is the emissions counterpart of the cost-of-energy finding [1] that auxiliary energy costs fall faster than propulsion energy costs under electrification.

# 3 Numerical results

## 3.1 Reduction surface

Figure 4 shows the full reduction surface $R(g, s)$ with the break-even contour, intermediate reduction levels, and representative national grid factors annotated at $s = 0$. Table 1 provides numerical values at discrete points.

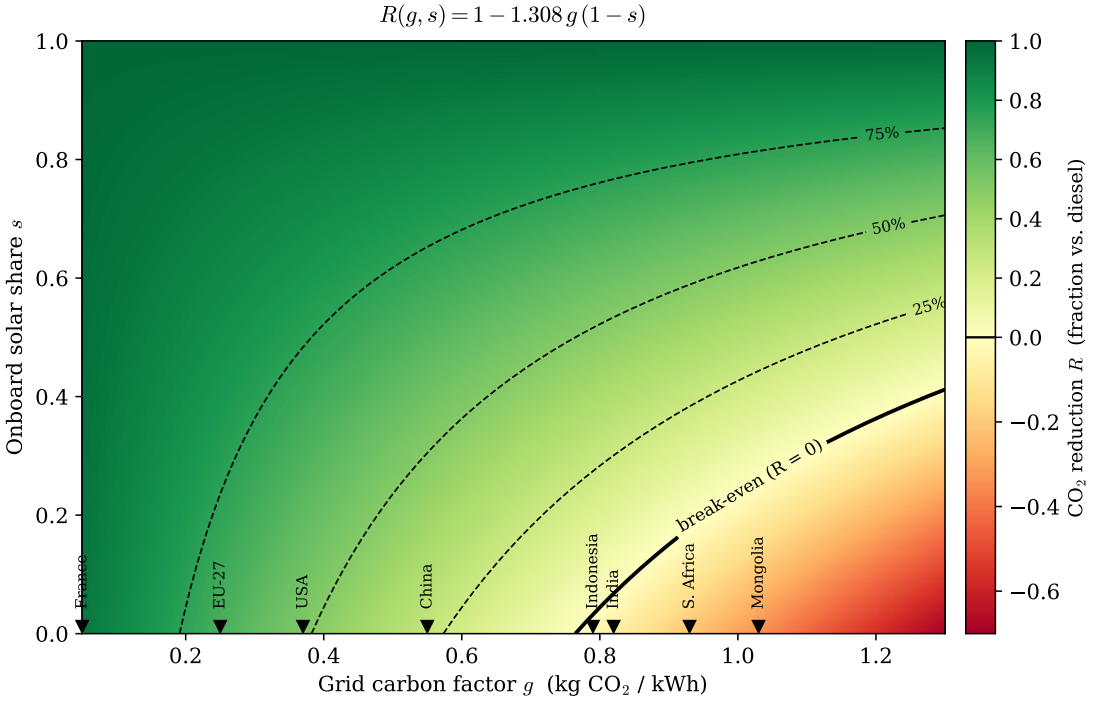


Figure 4: $CO_2$ reduction surface $R(g, s) = 1 - 1.308 \cdot g \cdot (1 - s)$. The solid black contour marks the break-even ($R = 0$); dashed contours mark intermediate reduction levels (25%, 50%, 75%). National grid factors are annotated along $s = 0$. Negative values (red) indicate that electrification increases $CO_2$ relative to diesel.

Table 1: Annual $CO_2$ reduction $R$ (%) achieved by replacing a diesel ferry with a battery-electric ferry, as a function of grid carbon factor $g$ and solar share $s$. Negative values (in red) indicate that electrification increases $CO_2$ relative to diesel.

| $s \setminus g$ (kg $CO_2$/kWh) | 0.10 | 0.25 | 0.50 | 0.75 | 1.00 | 1.20 |
|---|---|---|---|---|---|---|
| 0.00 | +87% | +67% | +35% | +2% | –31% | –57% |
| 0.10 | +88% | +71% | +41% | +12% | –18% | –41% |
| 0.25 | +90% | +75% | +51% | +26% | +2% | –18% |
| 0.50 | +93% | +84% | +67% | +51% | +35% | +22% |
| 0.75 | +97% | +92% | +84% | +75% | +67% | +61% |
| 1.00 | +100% | +100% | +100% | +100% | +100% | +100% |

## 3.2 Representative grid mixes

Table 2 places national grid factors against the break-even threshold at zero and modest solar shares. This complements the country-level cost analysis of [1], which ranked 133 countries by the diesel–grid cost spread; here I rank by carbon spread instead.

Table 2: Selected grid carbon factors and resulting $CO_2$ reduction $R$ at $s = 0$ (no onboard solar) and $s = 0.25$. Grid factors are 2022–2024 averages on a life-cycle (well-to-wake) basis from IEA [9, 10] unless otherwise noted.

| Country / region | $g$ (kg $CO_2$/kWh) | $R$ at $s = 0$ | $R$ at $s = 0.25$ |
|---|---|---|---|
| Norway (hydro) | 0.02 | +97% | +98% |
| Sweden | 0.04 | +95% | +96% |
| France (nuclear) | 0.05 | +93% | +95% |
| EU 27 average | 0.25 | +67% | +75% |
| United States | 0.37 | +52% | +64% |
| China | 0.55 | +28% | +46% |
| Indonesia | 0.79 | –3% | +22% |
| India | 0.82 | –7% | **+20%** |
| South Africa | 0.93 | –22% | +9% |
| Mongolia | 1.03 | –35% | –1% |

### 3.3 Three regimes

The reduction surface partitions naturally into three regimes:

1. **Clean grid ($g < 0.76$).** Electrification reduces $CO_2$ at any solar share, including $s = 0$. Solar contributes marginal benefit. Examples: Nordic countries, France, the EU-27 average, the United States, and China. Operators in these regions can defer solar deployment without compromising the $CO_2$ case.

2. **Medium grid ($0.76 \leq g < 0.95$).** Electrification $CO_2$ benefits depend on solar share. At $s = 0$ the case is marginally negative; even a modest $s \approx 0.10$–$0.25$ turns it favorable. India and Indonesia fall in this regime. The $CO_2$ case for electrification is contingent on either solar augmentation or anticipated grid decarbonization. This parallels the OPEX finding in [1] that India is marginally attractive for direct electrification, with solar providing a strong tilt toward viability — empirically demonstrated for the solar ferry ADITYA in [5].

3. **Dirty grid ($g \geq 0.95$).** Electrification with negligible solar increases $CO_2$ relative to diesel. A solar share above ∼25%–30% is required to recover parity. South Africa, Mongolia, Kazakhstan, and coal-only sub-grids fall in this regime. Until significant grid decarbonization or larger solar installations are feasible, alternative pathways (e.g. green hydrogen, biodiesel, hybrid configurations) may be more $CO_2$-effective than direct battery electrification.

## 4 Sensitivity to physical assumptions

The numerical constants in equation (6) depend on three inputs: motor efficiency $\eta_M$, diesel SFC, and the diesel emission factor $f_d$. Table 3 shows the sensitivity of the break-even threshold $R_0 = g(1 - s)$ to plausible variation in each.

Two observations:

- The break-even threshold is robust to motor efficiency variation: a 5% improvement in the motor shifts $R_0$ by less than 6%.

- The choice of diesel emission factor matters more. The baseline uses a well-to-wake factor ($f_d = 3.20$ kg/L); a combustion-only tank-to-wake factor (∼2.68 kg/L, some 15%–20% lower) shifts $R_0$ from 0.76 down to ∼0.64. On the well-to-wake basis electrification is

Table 3: Break-even threshold $R_0 = g(1 - s)$ under variation of physical assumptions.

| Parameter | Range | $R_0$ |
|---|---|---|
| Baseline (WTW) | $\eta_b\eta_e\eta_M = 0.812$, SFC = 250, $f_d = 3.20$ | 0.76 |
| High-efficiency motor | $\eta_M = 0.95$ (chain = 0.857) | 0.68 |
| Older diesel engine | SFC = 280 g/kWh | 0.72 |
| Large marine engine | SFC = 175 g/kWh | 0.54 |
| Lower emission factor | $f_d = 2.50$ kg $CO_2$/L | 0.60 |
| Lifecycle diesel (well-to-wake) | $f_d = 3.20$ kg $CO_2$/L [11] | 0.76 |

favorable across a wide range of grids — China ($g = 0.55$) comfortably so — and India ($g = 0.82$) sits only marginally negative without solar.

Both sides of the comparison are on a consistent well-to-wake basis: the diesel factor includes upstream fuel production, and the grid factors include upstream generation losses.

# 5 Methods

The closed-form expression in equation (6) was derived analytically from first principles, but its parameter values and the regime boundaries were verified numerically against a multi-scenario ferry techno-economic model implemented by the author [13], building directly on the cost-of-energy framework established in [1] and extended here to emissions. The model resolves daily mechanical propulsion energy from the speed-power curve, daily auxiliary load, motor and inverter efficiencies, and solar generation derated for insolation and inverter efficiency. It outputs annual energy demand from grid, diesel, and onboard solar for each of eight propulsion architectures, and from these computes annual $CO_2$ emissions using user-set emission factors.

To verify the cancellation of vessel-specific terms in equation (6), the model was run across a parameter sweep spanning vessel speeds (8–14 knots), daily ranges (75–200 km), and annual operating days (200–350). For each combination, the reduction $R$ predicted by equation (6) agreed with the model output to within 0.5 % across all $(g, s)$ combinations evaluated, confirming that the residual dependence on $E_{\text{mech}}$ in the model arises only from second-order rounding effects (integer cylinder counts in the diesel pathway and integer kWh battery sizes).

Sensitivity values in Table 3 were computed by direct substitution into equation (5) with the named parameter varied and others held at baseline. National grid carbon factors in Table 2 are 2022–2024 average values on a life-cycle (well-to-wake) basis reported by the International Energy Agency [9, 10]; values for sub-national or peak-hour conditions may differ substantially.

The heatmap in Figure 4 was generated by direct evaluation of equation (6) on a $200 \times 200$ grid spanning $g \in [0.05, 1.30]$ and $s \in [0.0, 1.0]$, with contour lines plotted at $R = 0, 0.25, 0.50, 0.75$. The plotting code, the underlying ferry model, and an interactive calculator are available from the author on request.

The analysis uses well-to-wake accounting for operational energy on both sides, but excludes embodied emissions of battery, motor, power-electronics, and PV manufacture; including these would shift the absolute numerical constants in equation (6) but does not change the structural form of the inequality or the regime partition.

# 6 Implications and limitations

Equation (6) is intentionally simple. Several factors are excluded from the analysis:

- **Embodied emissions** of batteries, motors, power electronics, and PV modules. The component-level life-cycle assessment in [6, pp. 25–26] finds that the production emissions

of the solar array and battery are recovered within roughly one year of operation, so over a multi-decade life they are a small fraction of cumulative operational emissions. Including them would shift $R$ downward by a vessel-life-dependent amount, but does not change the qualitative regime structure.

- **Auxiliary loads** (HVAC, hotel power) are treated separately in Section 2.5. Because the diesel reference meets these electrical loads through a generator set, their $CO_2$ comparison is more favourable to electrification than propulsion — the auxiliary break-even ($g(1-s) \approx 0.94$) sits well above the propulsion value (0.76) — so a vessel with a significant auxiliary share tolerates a somewhat dirtier grid than equation (6) alone would suggest.
- **Solar plant degradation**, which reduces effective $s$ over vessel life by roughly 0.5%–1% per year [12].
- **Hybrid configurations** (serial and parallel diesel-electric), which fall between the diesel and pure-electric cases. The same framework applies with $g \to g_{\text{eff}}$ defined as a weighted average of grid and onboard diesel-derived electricity. As shown in [1], parallel hybrid configurations achieve lower OPEX than series hybrids; the same direct-drive efficiency advantage carries through to $CO_2$ emissions.

The most consequential omission is **temporal grid factor variation**. Equation (6) treats $g$ as a constant, but grid carbon intensity varies by hour and season. Ferry charging schedules that align with low-carbon grid periods (overnight nuclear/wind windows in some regions) achieve effective $g$ values 30%–50% lower than the annual average. This temporal optionality is a significant advantage for electrification that the present analysis does not capture.

A further qualifier: the framework treats solar as a perfect substitute for grid energy on a kWh basis. In practice, the solar share $s$ that can be realized depends on PV plant sizing relative to vessel demand, insolation, system efficiency, and a derating factor accounting for low-sun periods that the battery must cover from grid energy. A 25 kW PV array on a 1,900 kWh/d ferry yields $s$ typically below 5% under realistic derating assumptions. Achieving $s = 0.25$ on a typical coastal ferry requires PV capacity in the range of 100–400 kW depending on derate and operating profile, which may exceed available deck area. The practical design, PV sizing, and operation of such solar-electric vessels are treated in detail in [6].

# 7 Conclusion

The $CO_2$ reduction achieved by replacing a diesel passenger ferry with a battery-electric ferry can be expressed in closed form as $R = 1 - 1.308 \cdot g \cdot (1 - s)$. The result is independent of vessel size, route, and operating profile, depending only on grid carbon factor $g$ and onboard solar share $s$. Three regimes emerge:

- On grids with $g < 0.65$ kg $CO_2$/kWh, electrification reduces $CO_2$ regardless of solar share.
- On grids with $0.65 \leq g < 0.85$, the $CO_2$ case requires modest solar augmentation ($s \gtrsim 0.25$) or anticipated grid decarbonization.
- On grids with $g \geq 0.85$, substantial solar ($s > 0.35$) is necessary for $CO_2$ parity; alternative pathways may be preferable until grid decarbonization or larger PV installations become feasible.

These $CO_2$ regimes are not identical to the OPEX regimes derived in [1] but they share the same vessel-independent structure, governed by an externally-fixed cost factor (diesel price or carbon factor) and a vessel-controllable mitigation lever (solar share). The framework supports

rapid screening of ferry electrification cases against regional grid conditions, and provides a simple test for when solar augmentation is essential versus optional. Future work should extend the analysis to lifecycle (well-to-wake) accounting, hybrid configurations, and temporally-resolved grid factors.

## Acknowledgements

The author thanks colleagues who reviewed earlier drafts of this note.

## References

[1] S. Thandasherry, "Cost of energy in a vessel: assessing likely applications in marine transport where shift to electric will succeed without other interventions," *Proc. International Conference on Green Technologies in Coastal and Inland Water Transportation (GTCIWT)*, 2024.

[2] A. Kortsari, L. Mitropoulos, T. Heinemann, H. Mikkelsen, and G. Aifadopoulou, "Evaluating the economic performance of a pure electric and diesel vessel: the case of E-ferry in Denmark," *Transactions on Maritime Science*, vol. 11, no. 1, pp. 95–109, 2022.

[3] F. M. Kanchiralla, E. Grunditz, A. Nordelöf, S. Brynolf, and E. Wikner, "Environmental and economic assessment of electric ferries with different lithium-ion battery technologies," *Applied Energy*, vol. 396, art. 126274, 2025.

[4] R. Otsason and U. Tapaninen, "Decarbonizing city water traffic: case of comparing electric and diesel-powered ferries," *Sustainability*, vol. 15, no. 23, art. 16170, 2023.

[5] S. Thandasherry, "Economics of ADITYA — India's first solar ferry," *IEEE India Info*, pp. 38–45, Jul–Sep 2018.

[6] S. Thandasherry, *Solar-Electric Boats: Plan, Build and Benefit*, 2021. ISBN 979-8530106996.

[7] International Maritime Organization, *2024 Guidelines on Life Cycle GHG Intensity of Marine Fuels (2024 LCA Guidelines)*, Resolution MEPC.391(81), adopted 22 March 2024.

[8] IPCC, *2006 IPCC Guidelines for National Greenhouse Gas Inventories, Volume 2: Energy*, Intergovernmental Panel on Climate Change, 2006.

[9] IEA, *Emissions Factors 2024*, International Energy Agency, Paris, 2024.

[10] IEA, *Life Cycle Upstream Emissions Factors 2024*, International Energy Agency, Paris, 2024.

[11] JEC (JRC–EUCAR–CONCAWE), *Well-to-Tank Report Version 4.a: Well-to-Wheels Analysis of Future Automotive Fuels and Powertrains in the European Context*, EUR 26237 EN, ISBN 978-92-79-33888-5, Publications Office of the European Union, Luxembourg, 2014.

[12] D. C. Jordan and S. R. Kurtz, "Photovoltaic degradation rates — an analytical review," *Progress in Photovoltaics: Research and Applications*, vol. 21, no. 1, pp. 12–29, 2013.

[13] S. Thandasherry, *Ferry techno-economic model and $CO_2$ comparator*, Navalt internal tool, 2026. Available on request.

# A Nomenclature

| Symbol | Meaning | Units |
|---|---|---|
| $E_{\text{mech}}$ | Annual mechanical propulsion energy | kWh/yr |
| SFC | Specific fuel consumption (diesel engine) | g/kWh |
| $\rho$ | Diesel density | kg/L |
| $f_d$ | Diesel well-to-wake $CO_2$ emission factor | kg $CO_2$/L |
| $\eta_M$ | Electric motor efficiency | — |
| $\eta_e$ | Onboard electrical / power-conversion efficiency | — |
| $\eta_b$ | Battery efficiency | — |
| $\eta_A$ | Genset alternator efficiency | — |
| $g$ | Grid electricity carbon factor | kg $CO_2$/kWh |
| $s$ | Solar share of daily energy demand | — |
| $R$ | $CO_2$ reduction vs diesel | — |
| $R_0$ | Break-even threshold for $g(1-s)$ | — |

# B Derivation of equations (6) and (8)

### Propulsion

Starting from equations (1) and (3):

$$R = 1 - \frac{\text{CO}_2^{\text{electric}}}{\text{CO}_2^{\text{diesel}}} = 1 - \frac{\dfrac{E_{\text{mech}}}{\eta_b \eta_e \eta_M}(1-s)g}{E_{\text{mech}} \cdot \dfrac{\text{SFC} \cdot f_d}{1000 \cdot \rho}}$$

The $E_{\text{mech}}$ terms cancel:

$$R = 1 - \frac{(1-s)g}{\eta_b \eta_e \eta_M} \cdot \frac{1000\rho}{\text{SFC} \cdot f_d}$$

Substituting $\eta_b \eta_e \eta_M = 0.95 \times 0.95 \times 0.90 = 0.812$, $\rho = 0.85$ kg/L, SFC $= 250$ g/kWh, $f_d = 3.20$ kg/L:

$$R = 1 - \frac{(1-s)g}{0.812} \cdot \frac{1000 \cdot 0.85}{250 \cdot 3.20} = 1 - 1.308 \cdot (1-s) \cdot g$$

Setting $R = 0$ gives the break-even condition $g(1-s) = 1/1.308 = 0.764$.

### Auxiliary loads

Auxiliary loads are electrical on both vessels, so the derivation is set on a delivered electrical-energy basis $E_{\text{aux}}$. On the diesel vessel they are supplied by a generator set: the engine produces mechanical energy at the same carbon intensity as above, $\text{SFC} \cdot f_d/(1000\,\rho)$ per kWh mechanical, and an alternator of efficiency $\eta_A$ converts it to electricity. Delivering $E_{\text{aux}}$ of electrical energy therefore requires $E_{\text{aux}}/\eta_A$ of mechanical energy:

$$\text{CO}_2^{\text{aux, diesel}} = \frac{E_{\text{aux}}}{\eta_A} \cdot \frac{\text{SFC} \cdot f_d}{1000\,\rho}.$$

The battery-electric vessel draws $E_{\text{aux}}$ through the battery (efficiency $\eta_b$) and onboard electrical system (efficiency $\eta_e$), supplied by grid and solar; the propulsion motor is not in the path, so only $\eta_M$ drops out:

$$\text{CO}_2^{\text{aux, electric}} = \frac{E_{\text{aux}}}{\eta_b\,\eta_e} \cdot (1-s)\,g.$$

Forming $R_{\text{aux}} = 1 - \text{CO}_2^{\text{aux, electric}} / \text{CO}_2^{\text{aux, diesel}}$, the $E_{\text{aux}}$ terms cancel and the diesel fraction inverts (moving $\eta_A$ to the numerator):

$$R_{\text{aux}} = 1 - \frac{\dfrac{E_{\text{aux}}}{\eta_b\,\eta_e}(1-s)\,g}{\dfrac{E_{\text{aux}}}{\eta_A} \cdot \dfrac{\text{SFC} \cdot f_d}{1000\,\rho}} = 1 - \frac{\eta_A}{\eta_b\,\eta_e} \cdot \frac{1000\,\rho}{\text{SFC} \cdot f_d} \cdot (1-s)\,g.$$

Substituting $\eta_A = 0.90$, $\eta_b = \eta_e = 0.95$, and the same $\rho$, SFC, $f_d$:

$$R_{\text{aux}} = 1 - \frac{0.90}{0.95 \times 0.95} \cdot \frac{1000 \cdot 0.85}{250 \cdot 3.20} \cdot (1-s)\,g = 1 - (0.997 \times 1.063) \cdot (1-s)\,g = 1 - 1.06 \cdot (1-s)\,g.$$

Setting $R_{\text{aux}} = 0$ gives the auxiliary break-even $g(1-s) = 1/1.06 = 0.94$. Comparing the two constants, the propulsion drivetrain divides by $\eta_b\eta_e\eta_M = 0.812$ whereas the auxiliary path divides only by $\eta_b\eta_e = 0.9025$ and multiplies by $\eta_A$; this replacement of the motor term by the alternator term is what raises the tolerable grid factor from 0.76 to 0.94.